Journal of Materials Chemistry A

Accepted Manuscript

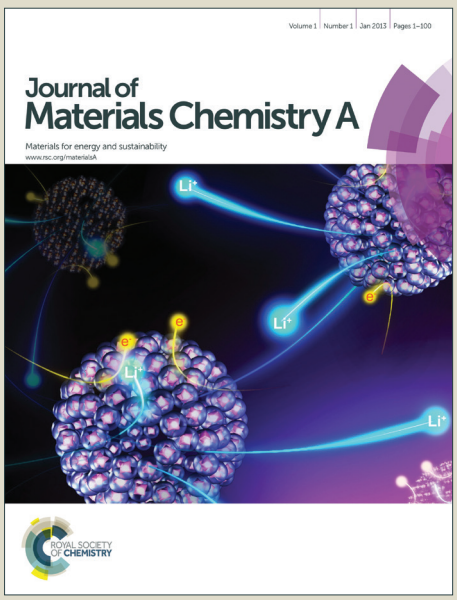

ROYAL SOCIETY OF CHEMISTRY

www.rsc.org/materialsA

Cite this: DOI: 10.1039/c0xx00000x

www.rsc.org/xxxxxx

ARTICLE TYPE

Facile one step method realizing scalable production of g-C_3N_4 nanosheets and study of their photocatalytic H_2 evolution activity

Xiuli Lu,‡ Kun Xu,‡ Pengzuo Chen, Kaicheng Jia, Si Liu, Changzheng Wu*

Received (in XXX, XXX) XthXXXXXXXXX 20XX, Accepted Xth XXXXXXXXX 20XX

DOI: 10.1039/b000000x

Graphene-like g-C_3N_4 nanosheets show great potential application in varied fields owing to their unique electronic and optical properties. However, most of the developed methods for preparing g-C_3N_4 nanosheets still suffered from low-yield and time-consuming shortcomings, which greatly hampered their further study and application. Herein, a facile dicyandiamide-blowing method with NH_4Cl as the gas template for synergic achievement of large-quantity and high-quality graphene-like g-C_3N_4 nanosheets has been reported. The g-C_3N_4 nanosheets prepared by this one step method possess enhanced specific area surface, improved electron transport ability and increased lifetime of photoexcited charge carriers, bringing enhanced photocatalytic H_2 activities than that of bulk g-C_3N_4. Our work represents a significant progress for scalable fabrication of high quality 2D g-C_3N_4 and provides a new pathway for scalable production of 2D nanomaterials.

Introduction

During past few years, two dimensional (2D) graphene has gained more and more attention due to its unique 2D confined structure, bringing about exotic properties such as excellent electronic, thermal and mechanical properties.[1-3] As the expansion in the field of graphene, ultrathin 2D nanosheets of transition metal oxides,[4-6] metal chalcogenides,[7,8] nitride[9] and transition metal phosphates[10] have also been widely explored and show great advantages in energy storage devices,[11] sensors,[12] stamp-transferrable electrodes,[13] electronics[14] and catalysis.[15] Typically, various methods mainly including the strategy of mechanical cleavage,[16] liquid exfoliation,[17] lithium intercalation-deintercalation of layer-structure materials,[18] oriented attachment,[19] and topochemical transformation strategy[20] have been devoted to the synthesis of 2D ultrathin nanosheets.

Graphite carbon nitride (g-C_3N_4), a typical layered structure, is well known as a nontoxic metal-free semiconductor,[21-23] which has been studied as a perspective material in varied areas, such as wastewater detoxification,[24] CO_2 reduction,[25,26] catalytic,[15] hydrogen/oxygen evolution through water splitting.[21] Motivated by graphene, great efforts have recently been devoted to preparing g-C_3N_4 ultrathin nanosheets and researching their novel properties. For instance, g-C_3N_4 nanosheets can be obtained by a "green'' liquid exfoliation route from bulk g-C_3N_4 in water and exhibit as a promising candidate for bioimaging application.[27] What is more, the g-C_3N_4 nanosheets synthesized through simple liquid-phase exfoliation in various solvent and thermal oxidation "etching" process of bulk g-C_3N_4, also show significantly enhanced photocatalytic H_2 activities.[28,29] Unfortunately, most of current methods to fabricate g-C_3N_4 nanosheets are usually low-yield and time-consuming. In view of significance of 2D g-C_3N_4 nanosheets, new alternative way to obtain g-C_3N_4 nanosheets with high quality and large quantity is still much necessary.

Herein, we report a facile one step method for synergic achievements of large-quantity and high-quality few-layer graphene-like g-C_3N_4 nanosheets. The raw materials of our reported simple approach were dicyandiamide and ammonium chloride. And during the reaction process, the chemically released gases from ammonium chloride blew dicyandiamide-derived polymers into numerous large bubbles, with g-C_3N_4 nanosheets obtained. This method has the merits of low-cost, scalable production and high efficiency. The g-C_3N_4 nanosheets with 3.1 nm thickness possess enhanced specific surface area and achieve improved electron transport ability as well as efficient separation rate of the electron and hole. As expected, the g-C_3N_4 nanosheets produced by the facile dicyandiamide-blowing method deliver the hydrogen evolution rate of 450 μ $molh^{-1}$, which is more than ten times larger than that of the bulk g-C_3N_4. The work not only provides a facile strategy for synthesis of 2D g-C_3N_4, but also paves a new way for the scalable production of other 2D materials.

Experimental

Synthesis of bulk and nanosheets of g-C_3N_4

Bulk g-C_3N_4 powder was synthesized according to the previous paper.[29] Typically, 2 g of dicyanodiamide powder was put into crucible and heated at 550℃ for 4h at a rate of 3℃/min.

The resultant yellow material was milled into powder in a mortar for further investigations. For preparation of the g-C_3N_4 nanosheets, 2 g of dicyanodiamide powder and 10 g ammonium chloride were fully mixed (The "fully mixed "was the key for the success of the experiment.) In fact, NH_4Cl, acts as supplementary material, which could provide dynamic gas template, benefiting to the formation of the ultrathin graphene-like g-C_3N_4. The mixture was heated at 550℃ for 4h. The resultant materials were characterized as g-C_3N_4 nanosheets.

Materials Characterization

The samples were characterized by X-ray powder diffraction (XRD) by a Philips X'Pert Pro Super diffractometer equipped with graphite-monochromatized Cu-Kα radiation (λ=1.54178Å). Tapping-mode atomic force microscopy (AFM) images were obtained on DI Innova Multimode SPM platform. Transmission electron micros-copy (TEM) images were carried out on H-7650 (Hitachi, Japan) operated at an acceleration voltage of 100 kV. The Fourier transform infrared (FT-IR) experiment was taken on a Magna-IR750 FT-IR spectrometer in a KBr pellet, scanning from 4000 to 400 cm^{-1}. X-ray photoelectron spectroscopy (XPS) measurements were performed on a VG ESCALAB MK II X-ray photoelectron spectrometer with an exciting source of Mg Kα = 1253.6 eV. UV-Vis-NIR absorption spectra were recorded on a Perkin Elmer Lambda 950 UV/Vis-NIR spectrophotometer. The photoluminescence (PL) spectrum was performed by FLUOROLOG-3-TAU fluorescence spectrometer equipped integrating sphere. The ns-level time-resolved PL spectra were performed by FLS920, Edinburgh Instruments Ltd. The photocurrent and EIS (electro-chemical impedance spectroscopy) response was measured with three electrodes, of which the Ag/AgCl and Pt electrodes were used as the counter and reference electrode, respectively.

Photocatalytic Activity Measurements

Water-splitting reactions were carried out in a top-irradiation vessel connected to a glass closed gas circulation system. 50 mg of bulk g-C_3N_4 or g-C_3N_4 nanosheet was dispersed in 200 mL aqueous solution containing 10 vol% triethanolamine scavengers. The deposition of 3 wt% Pt co-catalyst was conducted by directly dissolving H_2PtCl_6 in the above 200 mL reaction solution. The amount of hydrogen evolution was determined using a gas chromatograph (Agilent 7890A).

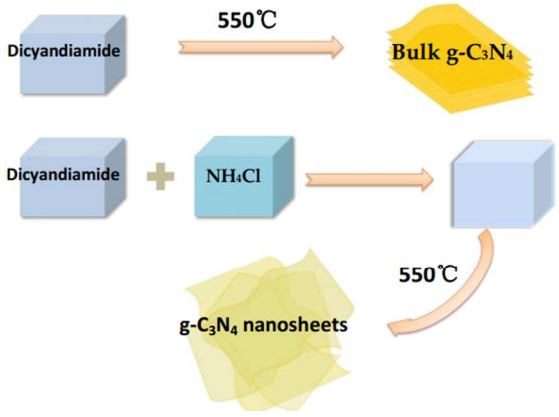

Figure 1. Schematic illustration of the synthesis process of the bulk and ultrathin nanosheets of g-C_3N_4.

Results and discussion

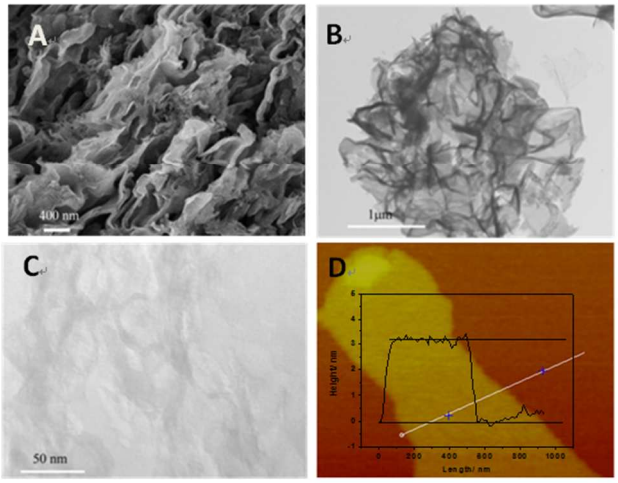

Figure 2. (A) The SEM image of graphene-like g-C_3N_4. (B) Low-resolution TEM image of the graphene-like g-C_3N_4. (C) High-resolution TEM image of the graphene-like. (F) AFM image shows the morphology of the g-C_3N_4 nanosheet and the highlight step height is 3.10 nm.

As clearly illustrated in Figure 1A, bulk g-C_3N_4 was prepared by heating dicyandiamide at 550℃ for 4h according to previous literatures.[29] Meanwhile, 2D g-C_3N_4 nanosheets were obtained by heating a mixture of dicyandiamide and ammonium chloride at 550 ℃ for 4h. Specially, with the increase of temperature, dicyandiamide was gradually polymerized whereas gases (NH_3 and HCl) released from NH_4Cl blew dicyandiamide-derived polymers into many large bubbles and resulted in crinkly 2D g-C_3N_4 nanosheets. For better description of the difference between g-C_3N_4 gained by heating dicyandiamide with and without NH_4Cl, the comparison of dispersion effect was clearly demonstrated in Figure S3 (A-B). The g-C_3N_4 nanosheets show much better dispersibility and stability. What is more, the volume of 2D g-C_3N_4 is much larger than that of bulk g-C_3N_4 with the same mass and the expansion of volume leads to colour fading as shown in Figure S3 (C). Obviously, the dynamic gas template introduced by NH_4Cl is high-efficiency and realizes scalable production of carbon nitride nanosheets with one step reaction only.

The morphology of as-prepared bulk g-C_3N_4 and 2D g-C_3N_4 nanosheets were investigated with scanning electron microscopy (SEM), transmission electron microscopy (TEM) and atomic force microscopy (AFM), respectively. Compared with bulk g-C_3N_4 with large particle outlook in Figure S5, the as-prepared 2D g-C_3N_4 nanosheets exhibited as a soft and loose material with a diameter size of several micrometres (Figure 2A and Figure S6). TEM image of 2D g-C_3N_4 in Figure 2B shows characteristic of ultrathin nanosheets with crinkly structure. High-magnification TEM image in Figure 2C demonstrated that the surface of g-C_3N_4 nanosheets is rough with many hollows. The phenomenon was easy to understand because of the continuous gases emitting during the formation of g-C_3N_4 materials. Atomic force microscopy (AFM) was conducted to gain more information about the morphology and thickness of nanosheets. Typical AFM image and the corresponding thickness analyses in Figure 2D

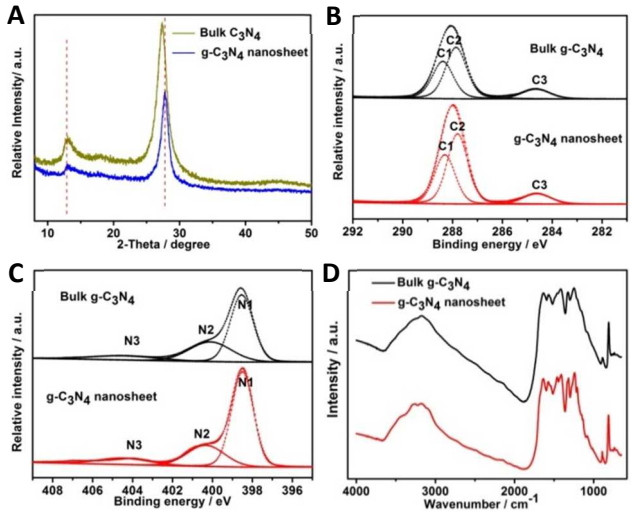

Figure 3. (A) The XRD patterns of the bulk g-C_3N_4 and the as-prepared g-C_3N_4 nanosheets. (B-C) High-resolution C 1s spectra and N 1s spectra of g-C_3N_4 nanosheets and bulk g-C_3N_4. (D) FTIR spectra of the bulk g-C_3N_4 and the as-prepared g-C_3N_4 nanosheets.

revealed ultrathin nanosheet morphology with uniform thickness of about 3.1 nm for as-obtained g-C_3N_4 sample. These morphologic characterization results clearly demonstrated that ultrathin g-C_3N_4 nanosheets were successfully synthesized by a facile dicyandiamide-blowing approach.

The crystal structure and compositions of the bulk and graphene-like g-C_3N_4 were analyzed by their X-ray diffraction (XRD) patterns, FTIR spectra and X-ray photoelectron spectra (XPS). As demonstrated in Figure 3A, XRD patterns of graphene-like g-C_3N_4 showed two distinct diffraction peaks, which were identical with bulk g-C_3N_4, indicating that the graphene-analogue g-C_3N_4 had the same crystal structure as the bulk g-C_3N_4. The strongest XRD peak (002) at about 27.3° is attributed to inter-planar stacking peak of aromatic systems. The low-angle reflection peak at 13.0°, derived from the lattice planes parallel to the c-axis. Compared with the bulk g-C_3N_4, the peak (002) in the g-C_3N_4 nanosheets is moved from 27.3° to 27.8°, and the corresponding value of d changed from 0.325 to 0.319 nm. This indicates a decreased gallery distance between the layers in the graphene-like carbon nitride, which could demonstrate that two-dimensional g-C_3N_4 nanosheets were formed during the heat treatment of the mixture of dicyandiamide and NH_4Cl.[29] To further probe the chemical composition and chemical states of bulk and the nanosheets of g-C_3N_4, XPS measurement was conducted. As shown in Figure S7, there was no obvious binding energy shift of N 1s and C 1s, exhibiting that the chemical states of both nitrogen and carbon in the g-C_3N_4 nanosheets were the same as in bulk g-C_3N_4. Specially, as shown in the high-resolution C 1s XPS spectra in Figure 3B, the peak at 288.4 eV (C1) and 287.8 eV (C2) could be assigned to the sp^2 C atoms bonded to N in the samples. The low peak located at 284.6 eV (C3) was related to carbon contamination. The similar intensity of the peak at 284.6 eV demonstrated that there was no obvious change of nitrogen content in g-C_3N_4 nanosheets. In addition, Figure 3C showed the high-resolution N 1s XPS spectra of the g-C_3N_4 nanosheets and bulk g-C_3N_4. It could be seen that N1s could be deconvoluted into three different peaks at 398.5 eV (N1), 399.9 eV (N2) and 404.0 eV (N3), demonstrating three types of N bonding in the samples. The dominant N 1s signal peak at 398.5 eV could be attributed to sp^2 hybridized nitrogen involved in triazine rings. The peak at a binding energy of about 399.9 eV were commonly assigned to bridging N atoms in tertiary nitrogen (N–(C)3) and terminal amino functions (C–N–H). The weak peak located at 398.5 eV (N3) could be attributed to positive charge localization or the charging effects in the cyano-group and hetero cycles.[28,29] According to the percentages of C and N determined by XPS analysis, it was found that the surface atomic ratio of C/N had increased from 0.77 (for the bulk g-C_3N_4) to 0.78 (for the graphene-like g-C_3N_4). The C/N ratio in g-C_3N_4 nanosheets is very close to that in bulk g-C_3N_4.

The structural information of the nanosheets were further confirmed by the FTIR spectra as shown in Figure 3D. There is no obvious difference between the characteristic FT-IR spectra of the as prepared bulk and nanosheets of g-C_3N_4, showing that the g-C_3N_4 nanosheets maintained same chemical structure as that in bulk g-C_3N_4. In detail, the broad peaks between 3600 and 3000 cm^{-1} are attributed to N–H stretching, exhibiting the partial hydrogenation of some N atoms in the 2D g-C_3N_4 nanosheets. The set of peaks between 1800 and 900 cm^{-1} are characteristic of trigonal C–N(–C)–C and bridging C–NH–C units.[30] From the above results, the crystal structure and chemical composition of the as prepared 2D g-C_3N_4 nanosheets are basically in conformity with that of the bulk g-C_3N_4.

Furthermore, their optical absorption spectra and fluorescence emission spectra were measured to study the electronic band structures of the bulk and nanosheets materials. The optical absorption of the as-prepared bulk g-C_3N_4 and g-C_3N_4 nanosheets samples were conducted by a UV-vis spectrometer and the results are demonstrated in Figure S8. Apparently, an obvious blue shift of the intrinsic absorption edge was found in UV-visible absorption spectra in the nanosheets

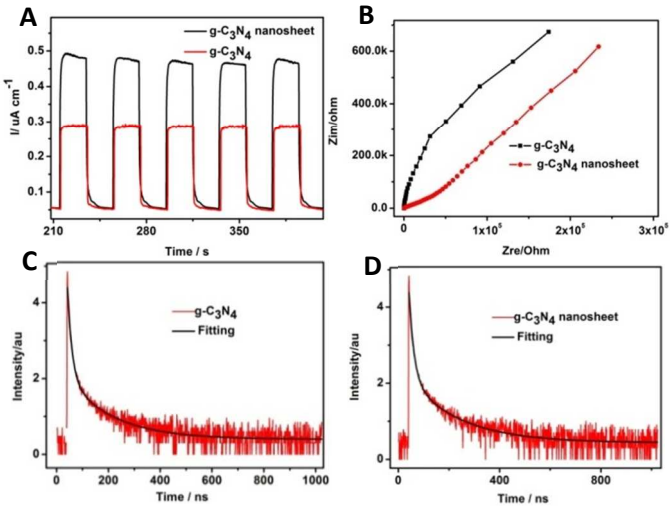

Figure 4. (A) The photocurrent density of g-C_3N_4 and g-C_3N_4nanosheets measured at 1 V bias voltage versus Ag/AgCl in 1 M Na_2SO_4 aqueous solution under illumination of a 300 W Xe lamp. (B) The EIS response of g-C_3N_4 and g-C_3N_4nanosheets electrode. (C-D) The ns-level time-resolved PL spectra monitored at 435 nm under 340 nm excitation for g-C_3N_4 and g-C_3N_4 nanosheets.

Table1 The fluorescence decay parameters in the bulk g-C_3N_4 and g-C_3N_4 nanosheets

	τ_1/ ns	A_1	τ_2/ns	A_2	$\langle\tau$/ns$\rangle$
g-C_3N_4	2.90	0.25	30.37	0.75	23.50
2D g-C_3N_4	2.75	0.24	31.97	0.76	25.07

relative to bulk g-C_3N_4. The derived bandgaps from the $(Ahv)^2$ versus photon-energy plots as shown in the Figure S8 are 2.83 eV and 2.73 eV for the g-C_3N_4 nanosheets and the bulk materials. The larger bandgap by 0.15 eV of the 2D g-C_3N_4 is further confirmed by the blue shift of the PL spectrum spectrum by ~15 nm as shown in Figure S9. The reason for this larger band gap is ascribed to the quantum confinement effect by shifting the valence and conduction bandedges in opposite directions.[31]

In order to understand the electronic interaction in the bulk g-C_3N_4 and g-C_3N_4 nanosheet, the photocurrent, electro-chemical impedance spectroscopy were tested. As shown in Figure 4A, the photocurrents were measured for several on-off cycles under illumination of a 300 W Xe lamp with bulk g-C_3N_4 and g-C_3N_4 nanosheets electrode. The photocurrent value decreased to zero when the irradiation of light was off and the photocurrent get back to a constant value as soon as the light was on, which was entirely reversible. It is well known that the photocurrent was the important evidence for demonstrating the charge separation and migration.[32] As clearly demonstrated, the photocurrent of g-C_3N_4 nanosheets electrodes was much larger than that of the bulk g-C_3N_4 electrode, demonstrating the improvement of the separation efficiency of photoinduced electrons and holes in g-C_3N_4 nanosheets.[32] The electro-chemical impedance spectroscopy, exhibited in Figure 4B, indicated the decreased electron-transfer resistance in g-C_3N_4 nanosheets, as the smaller diameter of the semicircular Nyquist plots.[28] To further understand the photophysical characteristics of photoexcited charge carriers, the ns-level time-resolved fluorescence decay spectra of g-C_3N_4 and g-C_3N_4 nanosheets were recorded, as shown in Figure 4 (C-D). The radiative lifetimes with different percentages could be determined as given in Table 1 by fitting the decay spectra. In

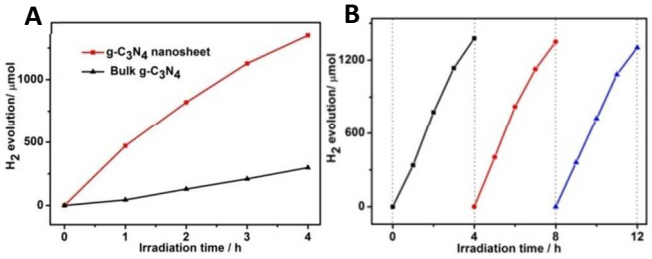

Figure 5. (A-B) A typical time course of hydrogen evolution from a water/triethanolamine solution.

detail, the short lifetime of 2.90 ns in g-C_3N_4 was decreased to 2.75 ns, with its percentage decreases from 25% to 24%. Both the long lifetime and percentage of charge carriers increase from 30.37 ns and 75% in the bulk to 31.97 ns and 76% in the nanosheets. As a result the weighted mean lifetime of 25.07 ns in g-C_3N_4 nanosheets was increased beyond 23.50 ns in g-C_3N_4. The increased lifetimes of charge carriers may be relevant to electron transport improvement and/or the changing electronic band structure arose from the quantum confinement effect in the nanosheets.[29] Thus, as the realization of graphene-like structure, the g-C_3N_4 nanosheets gained higher separation efficiency of electrons and holes, presenting potential application in photocatalytic area.

The photocatalytic activity of the g-C_3N_4 nanosheets is demonstrated in photocatalytic hydrogen evolution in a water/triethanolamine solution as shown in Figure 5. The average hydrogen evolution rate of the g-C_3N_4 nanosheets under illumination of a 300 W Xe lamp is 450 μ $molh^{-1}$, which is more than ten times larger than that of the bulk g-C_3N_4. Under illumination of a 300 W Xe lamp with a 420 nm cut-off filter (Figure S10), an average hydrogen evolution rate of the g-C_3N_4 nanosheets also show almost 13 times higher than that in bulk sample. The high activity of the photocatalyst was reproducible and the material showed good stability.

The enhancement of photocatalytic activity graphene in g-C_3N_4 nanosheets arises from synergistic effects of 2D structural configuration with ultrathin thickness of 3.1 nm, increased bandgap with about 0.15 eV, large surface area, improved electron transport ability and efficient separation rate of the electron and hole. The specific surface area of the g-C_3N_4 nanosheets was as high as 52.9 m^2g^{-1}, which was more than 19 times larger than that of the bulk g-C_3N_4 (2.9 m^2g^{-1}). (The N_2 sorption-desorption isotherm was shown in Figure S11). All the experimental results confirmed that 2D g-C_3N_4 nanosheets are synthesized successfully with high quality.

Conclusions

In conclusion, g-C_3N_4 nanosheets have been successfully synthesized by a facile dicyandiamide-blowing approach. NH_4Cl as the dynamic gas template was introduced in the solid-state reactions to prepare the ultrathin g-C_3N_4 nanosheets. The as-obtained nanosheets have synergic advantages of small sheet thickness, a large surface area, increased band gap and improved properties of photocatalytic reaction. Our experimental results represented significant progress in scalable fabrication of 2D g-C_3N_4 with high yield. The novel strategy presented here paves the way for bringing the g-C_3N_4 nanosheets to the broad applications and providing an inspiration for the scalable production of other 2D materials.

Acknowledgements

This work was financially supported by the National Natural Science Foundation of China (no. 21222101, 11132009, 21331005,11321503, J1030412), Chinese Academy of Science (XDB01010300), the Fok Ying-Tong Education Foundation, China(GrantNo.141042) and the Fundamental Research Funds for the Central Universities (no. WK2060190027 and WK2310000024).

Notes and references

Hefei National Laboratory for Physical Sciences at Microscale, Collaborative Innovation Center of Chemistry for Energy Materials, University of Science & Technology of China, Hefei, Anhui,230026, P.R. China. Tel: +86 551 63602455; E-mail: E-mail: czwu@ustc.edu.cn

† Electronic Supplementary Information (ESI) available: [details of any supplementary information available should be included here]. See DOI: 10.1039/b000000x/

‡ These authors contributed equally to this work.

1 L. Vicarelli, M. S. Vitiello, D. Coquillat, A. Lombardo, A. C. Ferrari,W. Knap, M. Polini, V. Pellegrini and A. Tredicucci, *Nat. Mater.*, 2012, **11**, 865.

2 C. Wu, J. Feng, L. Peng, Y. Ni, H. Liang, L. He and Y. Xie, *J. Mater. Chem.*, 2011, **21**, 18584.

3 A. K. Geim and K. S. Novoselov, *Nat. Mater.*, 2007, **6**, 183.

4 L. Peng, X. Peng, B. Liu, C. Wu, Y. Xie and G. Yu, *Nano Lett.*, 2013, **13**, 2151.

5 J. Zhu, Q. Li, W. Bi, L. Bai, X. Zhang, J. Zhou and Y. Xie, *J. Mater. Chem. A*, 2013, **1**, 8154.

6 X. Rui, Z. Lu, Z. Yin, D. H. Sim, N. Xiao, T. M. Lim, H. H. Hng, H. Zhang and Q. Yan, *Small*, 2013, **9**, 716.

7 M. Chhowalla, H. S. Shin, G. Eda, L.-J. Li, K. P. Loh and H. Zhang, *Nat. Chem.*, 2013, **5**, 263.

8 K. Xu, P. Chen, X. Li, C. Wu, Y. Guo, J. Zhao, X. Wu and Y. Xie, *Angew. Chem. Int. Ed.*, 2013, **52**, 10477.

9 M. Rousseas, A. P. Goldstein, W. Mickelson, M. A. Worsley, L. Woo and A. Zettl, *ACS Nano*, 2013, **7**, 8540.

10 D. Yang, Z. Lu, X. Rui, X. Huang, H. Li, J. Zhu, W. Zhang, Y. M. Lam, H. H. Hng, H. Zhang and Q. Yan, *Angew. Chem. Int. Ed.*, 2014, **126**, 9506.

11 C. Wu, X. Lu, L. Peng, K. Xu, X. Peng, J. Huang, G. Yu and Y. Xie,*Nat. Commun.*, 2013, **4**,2431.

12 Z. Jiang, J. Li, H. Aslan, Q. Li, Y. Li, M. Chen, Y. Huang, J. P. Froning, M. Otyepka, R. Zboril, F. Besenbacher and M. Dong, *J. Mater. Chem. A*, 2014, **2**, 6714.

13 C. Lin, X. Zhu, J. Feng, C. Wu, S. Hu, J. Peng, Y. Guo, L. Peng, J. Zhao, J. Huang, J. Yang and Y. Xie, *J. Am. Chem. Soc.*, 2013, **135**, 5144.

14 J. Feng, L. Peng, C. Wu, X. Sun, S. Hu, C. Lin, J. Dai, J. Yang and Y. Xie, *Adv. Mater.*, 2012, **24**, 1969.

15 X. She, H. Xu, Y. Xu, J. Yan, J. Xia, L. Xu, Y. Song, Y. Jiang, Q. Zhang and H. Li, *J. Mater. Chem. A*, 2014, **2**, 2563.

16 H. Li, G. Lu, Y. Wang, Z. Yin, C. Cong, Q. He, L. Wang, F. Ding, T. Yu and H. Zhang, *Small*, 2013, **9**, 1974.

17 J. N. Coleman, M. Lotya, A. O'Neill, S. D. Bergin, P. J. King, U. Khan, K. Young, A. Gaucher, S. De, R. J. Smith, I. V. Shvets, S. K. Arora, G. Stanton, H.-Y. Kim, K. Lee, G. T. Kim, G. S. Duesberg, T. Hallam, J. J. Boland, J. J. Wang, J. F. Donegan, J. C. Grunlan, G. Moriarty, A. Shmeliov, R. J. Nicholls, J. M. Perkins, E. M. Grieveson, K. Theuwissen, D. W. McComb, P. D. Nellist and V. Nicolosi, *Science*, 2011, **331**, 568.

18 Z. Zeng, T. Sun, J. Zhu, X. Huang, Z. Yin, G. Lu, Z. Fan, Q. Yan, H. H. Hng and H. Zhang, *Angew. Chem. Int. Ed.*, 2012, **51**, 9052.

19 C. Schliehe, B. H. Juarez, M. Pelletier, S. Jander, D. Greshnykh, M. Nagel, A. Meyer, S. Foerster, A. Kornowski, C. Klinke and H. Weller, *Science*, 2010, **329**, 550.

20 P. Chen, K. Xu, X. Li, Y. Guo, D. Zhou, J. Zhao, X. Wu, C. Wu and Y. Xie, *Chem. Sci.*, 2014, **5**, 2251.

21 X. Wang, K. Maeda, A. Thomas, K. Takanabe, G. Xin, J. M. Carlsson, K. Domen and M. Antonietti, *Nat. Mater.*, 2009, **8**, 76.

22 W. B. Zhang Jinshui, Wang Xinchen, *Progress in Chemistry*, 2014, 26, 19-29.

23 J. Chen, S. Shen, P. Guo, P. Wu and L. Guo, *J. Mater. Chem. A*, 2014, 2, 4605-4612.

24 Y. Cui, Z. Ding, X. Fu and X. Wang, *Angew. Chem. Int. Ed.*, 2012, **51**, 11814.

25 F. Goettmann, A. Thomas and M. Antonietti, *Angew. Chem. Int.Ed.*, 2007, **46**, 2717.

26 G. Dong and L. Zhang, *J. Mater. Chem.*, 2012, **22**, 1160.

27 X. Zhang, X. Xie, H. Wang, J. Zhang, B. Pan and Y. Xie, *J. Am. Chem. Soc.*, 2012, **135**, 18.

28 S. Yang, Y. Gong, J. Zhang, L. Zhan, L. Ma, Z. Fang, R. Vajtai, X. Wang and P. M. Ajayan, *Adv. Mater.*, 2013, **25**, 2452.

29 P. Niu, L. Zhang, G. Liu and H.-M. Cheng, *Adv. Funct. Mater.*, 2012, **22**, 4763.

30 B. V. Lotsch, M. Döblinger, J. Sehnert, L. Seyfarth, J. Senker, O. Oeckler and W. Schnick, *Chem. Eur. J.*, 2007, **13**, 4969.

31 A. P. Alivisatos, *Science*, 1996, **271**, 933.

32 W. Bi, C. Ye, C. Xiao, W. Tong, X. Zhang, W. Shao and Y. Xie, *Small*, 2014, **10**, 2820.

Table of contents

We report a facile one step method for achieving g-C_3N_4 nanosheets with enhanced photocatalytic H_2 evolution activity.